1900–1911 *Nucleic Acids Research, 2006, Vol. 34, No. 6*
doi:10.1093/nar/gkl126

Molecular basis of the targeting of topoisomerase II-mediated DNA cleavage by VP16 derivatives conjugated to triplex-forming oligonucleotides

Maria Duca[1,2,3,4], Dominique Guianvarc'h[1,2,3,4], Kahina Oussedik[1,2,3,4], Ludovic Halby[1,2,3,4], Anna Garbesi[5], Daniel Dauzonne[6], Claude Monneret[6], Neil Osheroff[7,8], Carine Giovannangeli[1,2,3,4] and Paola B. Arimondo[1,2,3,4,*]

[1]UMR 5153 CNRS, Paris, France, [2]Muséum National d'Histoire Naturelle USM0503, Paris, France, [3]INSERM UR565, Paris, France, [4]43 rue Cuvier, 75231 Paris cedex 05, France, [5]Istituto di Sintesi Organica e Fotoreattività del Consiglio Nazionale delle Ricerche (ISOF-CNR) Via Gobetti 101, 40129 Bologna, Italy, [6]UMR 176 CNRS, Institut Curie, Section de Recherche, 26 rue d'Ulm 75248 Paris cedex 05, France, [7]Department of Biochemistry and [8]Department of Medicine (Hematology/Oncology), Vanderbilt University School of Medicine, Nashville TN 37232-0146, USA

Received November 24, 2005; Revised December 21, 2005; Accepted March 14, 2006

ABSTRACT

Human topoisomerase II (topo II) is the cellular target for a number of widely used antitumor agents, such as etoposide (VP16). These agents 'poison' the enzyme and induce it to generate DNA breaks that are lethal to the cell. Topo II-targeted drugs show a limited sequence preference, triggering double-stranded breaks throughout the genome. Circumstantial evidence strongly suggests that some of these breaks induce chromosomal translocations that lead to specific types of leukaemia (called treatment-related or secondary leukaemia). Therefore, efforts are ongoing to decrease these secondary effects. An interesting option is to increase the sequence-specificity of topo II-targeted drugs by attaching them to triplex-forming oligonucleotides (TFO) that bind to DNA in a highly sequence-specific manner. Here five derivatives of VP16 were attached to TFOs. The active topo II poisons, once linked, induced cleavage 13–14 bp from the triplex end where the drug was attached. The use of triple-helical DNA structures offers an efficient strategy for targeting topo II-mediated cleavage to DNA specific sequences. Finally, drug–TFO conjugates are useful tools to investigate the mechanistic details of topo II poisoning.

INTRODUCTION

Human topoisomerase II (topo II) is a ubiquitous nuclear enzyme involved in the control of DNA topology (1–4). During the catalytic cycle, the enzyme transiently cleaves dsDNA, passes an intact double helix through the break and reseals it. Vertebrates contain two isoforms of the enzyme, topo IIα and β (1). Topo IIα levels increase during cell proliferation and this enzyme appears to be the isoform involved in mitosis (2). To maintain DNA integrity during the strand passage event, the enzyme, a homodimer, forms a covalent 5′-phosphotyrosyl adduct between the catalytic Tyr^{804} of each monomer and a strand of the duplex. This covalent enzyme-cleaved DNA complex is referred to as the cleavage complex (1–4). Under normal physiological conditions, the DNA cleavage and ligation reactions of topoisomerase are tightly coordinated and the covalent intermediate is bearly detectable. However, a number of drugs, such as the antitumor etoposide (VP16) [for reviews (4–9)], block the religation step after DNA cleavage. As a result, they dramatically increase levels of topo II–DNA cleavage complexes (DNA/topo II/drug ternary complex). Although transient in nature, cleavage complexes are converted to permanent DNA strand breaks when nucleic acid tracking systems attempt to traverse the protein roadblock in the genetic material. The resulting DNA strand breaks initiate multiple recombination/repair pathways and can trigger cell death pathways (10,11).

Despite the wide use of topo II-targeted drugs as antitumor agents, several limitations hamper their benefits. Toxicity is

*To whom correspondence should be addressed. Tel: +33 1 40793859; Fax: +33 1 40793705; Email: arimondo@mnhn.fr
Present address:
Dominique Guianvarc'h, Synthèse, Structure et Fonction de Molécules Bioactives, Université Paris 6, CNRS UMR 7613, 4, place Jussieu, 75005 Paris, France

one limiting factor, and it is partially related to the fact that topo II poisons stimulate DNA cleavage at multiple sites along the double helix with a limited sequence preference (one or two bases around the cleavage site, e.g. C/T-1↓ for VP16). Moreover, the use of VP16 and other topo II poisons has been linked to the initiation of specific types of leukaemia that correlate with the generation of enzyme-mediated cleavage within the *MLL* gene (12–15). Therefore, an option to improve these agents would be to increase their sequence-specificity and to direct DNA cleavage only on a chosen target gene, involved, e.g. in tumor formation and/or maintenance.

The first attempt to increase the specificity of a topoisomerase-targeted drug used topo I poisons as a model system (16–18). These drugs act by stabilizing the topo I-DNA cleavage complex and increasing cleavage on one strand of the double helix (19). Sequence-specificity was enhanced considerably by linkage of topo I posions to a DNA recognition element, such as a triple helix-forming oligonucleotide (TFO). Camptothecin and rebeccamycin derivatives covalently linked to a TFO induce topo I-mediated DNA cleavage selectively near the triplex site (16–18).

In contrast, no specific targeting of the drug was observed upon attachment of amsacrine, a clinically-relevant topo II poison, to a TFO; rather, the only sequence-specific effect of the drug–TFO-conjugate on topo II binding and DNA cleavage was attributed to the changes in local DNA structure induced by the formation of the triple helix (20). Whether this lack of success resulted from the bulkiness of the enzyme, the geometry of the conjugate, or the local DNA sequence could not be determined. However, since amsacrine is a DNA intercalator, it could have been sequestered at the triplex/duplex junction and thus been unavailable for the enzyme.

Therefore, to further investigate the potential of TFO-poisons to selectively induce topo II-mediated DNA cleavage, several biologically active derivatives of VP16 were synthesized and linked to olignucleotides via terminal amino groups on the drug (21–23). Results reported in this work indicate that the conjugation of VP16 derivatives to TFOs is able to direct the action of topo II poisons and specifically induce DNA cleavage 14 bp from the terminus of the triplex site.

MATERIALS AND METHODS

Materials

^{1}H NMR spectra were recorded in chloroform-*d* or methanol-d_4, on a Bruker AC spectrometer (300 MHz). For all oligonucleotides (ODNs) conjugates, mass determination was accomplished by electrospray ionization on a Q-STAR pulsar I (Appleura) and high-performance liquid chromatography (HPLC) purifications were performed upon Agilent 1100 using a Waters XTerra MS® C_{18} reversed phase column (4.6 × 50 mm, 2.5 μm). Absorbance spectrophotometry was performed on an Uvikon 860 (Kontron).

All chemicals were purchased from Sigma–Aldrich, ICRF-193 from Euromedex. All solvents were of analytical grade. Analogs of VP16 **1**, **2**, **3** and **4** were synthesized as previously described (22,23) or **5** and **6** as described below. VP16 and analogs were dissolved in dimethylsulfoxide at 5 mM and then diluted further with water. They were attached to the TFOs end as described in Figure 1.

Topo II

Human topo IIα was purchased from NuVentures Ltd (UK) and mutant topo II Y805F was prepared as described previously (24).

Synthesis of 4-β-(4-Boc-aminomethylphenyl)amido-4′-O-demethyl-4′-O-(4-azidobenzoyl)-4-deoxypodophyllotoxin (5)

A solution of Boc-protected **4** was prepared as reported previously (23) (700 mg, 1.1 mmol) in anhydrous CH_2Cl_2 (50 ml) under inert atmosphere. p-Azidobenzoylchloride (235 mg, 1.3 mmol) and triethylamine (8 μl, 1.1 mmol) were added and the reaction mixture was stirred at room temperature for 3 h, according to (25). The medium was then taken up with CH_2Cl_2 and water. The organic phase was washed with H_2O (3 × 50 ml), then dried ($MgSO_4$) and filtered. This compound was purified by silica gel chromatography using CH_2Cl_2/acetone 90:10 to provide pure compound in 68% yield. R_f = 0.66 (CH_2Cl_2/acetone 90:10), ^{1}H NMR ($CDCl_3$) δ: 8.18 (d, 2H, J = 8.6 Hz, PhN_3), 7.72 (d, 2H, J = 8.1 Hz, PhCH_2NHBoc), 7.33 (d, 2H, J = 8.1 Hz, PhCH_2NHBoc), 7.11 (d, 2H, J = 8.6 Hz, PhN_3), 6.81 (s, 1H, 5-H), 6.57 (s, 1H, 8-H), 6.48-6.30 (m, 3H, 4-NH, 2′,6′-H), 5.98 (d, 2H, J = 4.2 Hz, CH_2O_2), 5.47-5.39 (m, 1H, 4-H), 4.98 (br s, 1H, NHBOC), 4.66 (d, 1H, J = 4.1 Hz, 1-H), 4.49 (t, 1H, J = 7.7 Hz, 11a-H), 4.31 (d, 2H, J = 5.6 Hz, CH_2NH), 3.87 (t, 1H, J = 4.8 Hz, 11b-H), 3.69 (s, 6H, 3′,5′-OCH_3), 3.10-2.92 (m, 2H, 2,3-H), 1.44 (s, 9H, Boc); MS (CI) *m*/*z*: 795 $[M + NH_4]^+$.

Synthesis of 4-β-(4-aminomethylphenyl)amido-4′-O-demethyl-4′-O-(4-azidobenzoyl)-4-deoxypodophyllotoxin (6)

Trifluoroacetic acid (TFA, 400 μl, 5.3 mmol) was added to a solution of **5** (400 mg, 0.53 mmol) in CH_2Cl_2 (10 ml). The reaction mixture was stirred for 5 h and washed with cold saturated $NaHCO_3$ followed by water until the pH of the solution was 6–7. The extract was dried over $MgSO_4$ and concentrated *in vacuo* at 30°C. The residue was purified by silica gel column chromatography using a mixture CH_2Cl_2/methanol 9:1 to afford the pure compound in 76% yield. R_f = 0.45 (CH_2Cl_2/methanol 9:1), ^{1}H NMR (CD_3OD) δ: 8.14 (d, 2H, J = 8.5 Hz, PhCH_2NH_2), 7.88 (d, 2H, J = 8.1 Hz, PhN_3), 7.49 (d, 2H, J = 8.1 Hz, PhN_3), 7.21 (d, 2H, J = 8.5 Hz, PhCH_2NH_2), 6.86 (s, 1H, 5-H), 6.59 (s, 1H, 8-H), 6.49 (s, 2H, 2′,6′-H), 5.97 (d, 2H, J = 1.8 Hz, CH_2O_2), 5.52-5.48 (m, 1H, 4-H), 4.73 (d, 1H, J = 5.2 Hz, 1-H), 4.47 (t, 1H, J = 8.0 Hz, 11a-H), 4.00 (s, 2H, CH_2NH), 3.87 (t, 1H, J = 9.8 Hz, 11b-H), 3.69 (s, 6H, 3′,5′-OCH_3), 3.40-3.28 (m, 1H, 2-H), 3.20-3.12 (m, 1H, 3-H); MS (CI) *m*/*z*: 695 $[M + NH_4]^+$.

ODNs

ODNs were purchased from Eurogentec and purified using quick spin Sephadex G-25 columns (BioRad). Concentrations were determined spectrophotometrically at 25°C using molar extinction coefficients at 260 nm calculated from a nearest-neighbor model (26). ODN, used as control, has the following sequence: 5′-TTTTMTTTTMMMMMMT-3′, where M stands for 5-methyl-2′-deoxycytidine.

Target duplex :

5′ GAATTCAAGCTTACACTCCCTATCAGTGATA **GAGAGAGAGAAAAAAA GAGA** AGATCTGAGCTCGGTACCCTAGGATC 3′
3′ CTTAAGTTCGAATGTGAGGGATAGTCACTAT **CTCTCTCTCTTTTTTT CTCT** TCTAGACTCGAGCCATGGGATCCTAG 5′

Oligonucleotides (TFO)

5′ MPMPMPMPMPPPPPPP 3′	16TFO
5′ MPMPMPMPMPPPPPPPPMPMP 3′	20TFO

Drug-TFO conjugates :

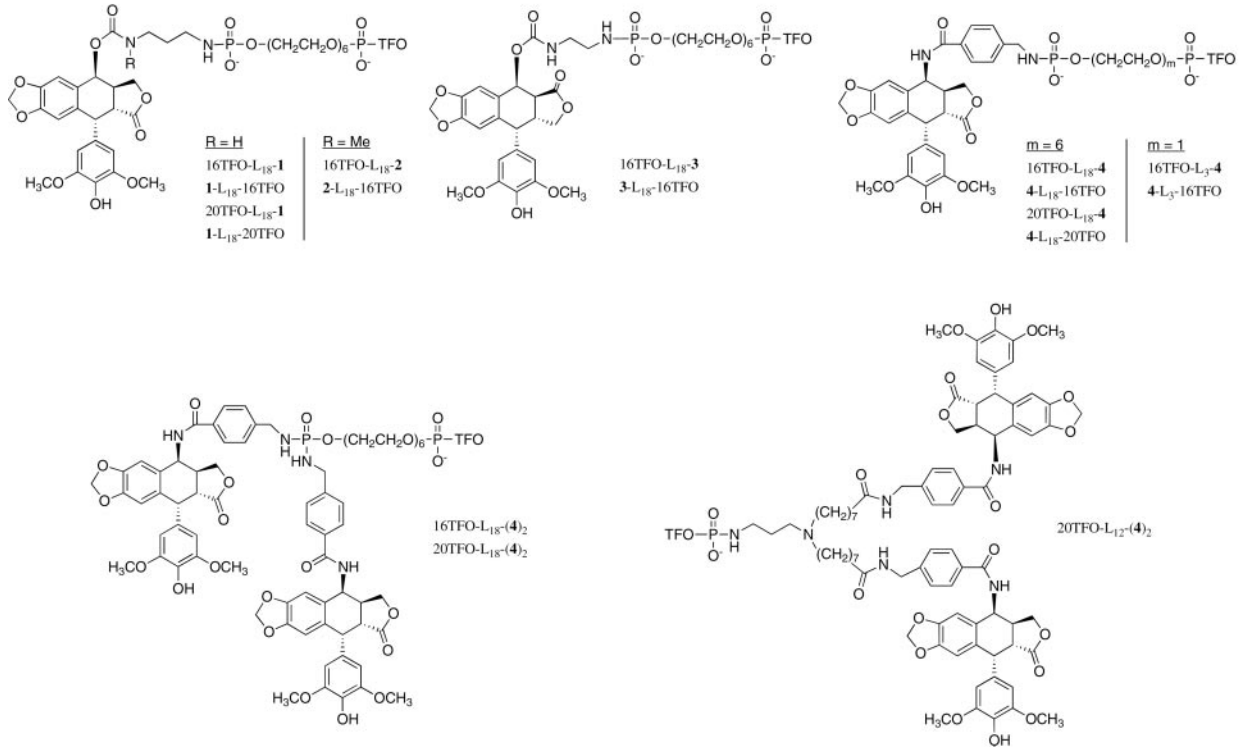

Figure 1. The sequence of the target duplex and the TFOs, and the chemical structure of the drug–TFO conjugates. The 77 bp duplex target sequence was inserted between the BamHI and EcoRI sites of pBSK. The TFO is complementary to the oligopurine strand of the duplex and binds parallel to it. The target site is in boldface for the 20 nt TFO and is underlined for the 16 nt TFOs. *M*, 5-methyl-2′-deoxycytidine; *P*, 5-propynyl-2′-deoxyuridine. The structures of the VP16 derivatives-TFO conjugates used in this study are shown. The nomenclature of the conjugates is described in the Materials and Methods.

The nomenclature of the ODNs and conjugates is the following: the abbreviation TFO is preceded by a number referring to the length of the ODN and followed, if attached to the 3′ end, or preceded, if attached through the 5′ end, by the letter L (for linker) and the number of atoms in the linker (L_3, ethylene glycol; L_{18}, hexaethylene glycol, L_{12}, 8-[(3-aminopropyl)-(7-carboxyheptyl)amino]octanoic acid), and finally, by the denomination of the 4′-demethylepipodophyllotoxin derivative. For example, 20TFO-L_{18}-**4** stands for the 20mer TFO linked at its 3′ end through the hexaethylene glycol spacer to compound **4**. The orientation of the triple helix is defined as the orientation of the purine-rich strand of the duplex, the TFO binds in the major groove in an orientation parallel to the oligopurine strand. All conjugates were synthesized and characterized as described in (23) or as described below.

Synthesis of 20TFO-L18-6 and 16TFO-L18-6

Azido compound **6** was attached to the terminal phosphate of the hexaethylene linker at the 3′ end of the TFOs according to the procedures described previously (27). The product was purified by HPLC and characterized by ultraviolet (UV) spectroscopy and mass spectrometry.

16TFO-L_{18}-**6** MS (ES^-) *m*/*z*: 6147 $[M-H]^-$ (calc. 6147)
20TFO-L_{18}-**6** MS (ES^-) *m*/*z*: 7410 $[M-H]^-$ (calc. 7410)

Plasmids and DNA fragments

The plasmid pBSK was purchased from Promega (USA) and the 77 bp target duplex was inserted between the BamHI and EcoRI sites (see Figure 1 for sequence). The 324 bp DNA fragment was prepared by 5′ ^{32}P-end-labeling the EcoRI or PvuII/alkaline phosphatase treated plasmid using [γ-^{32}P]ATP and T4 polynucleotide kinase followed by treatment with PvuII/EcoRI, yielding a fragment radiolabeled on the pyrimidine strand (Y) or on the purine strand (R), respectively. Digestion with NotI instead of PvuII generated 96 bp DNA fragments, alternatively 5′-radiolabeled on the Y or R strand. A 357mer DNA fragment was obtained by standard PCR using as alternatively 5′-radiolabeled primers 5′-CGAGGTCGACGGTATCGATAA-3′ and 5′-CACGACAGGTTTCCCGACTGG-3′, a temperature of annealing of 57°C and *Taq* I (Promega). The detailed procedure for isolation and purification has been described previously (28).

Topoisomerase II cleavage assays

The 5′ end 96 or 324 bp radiolabeled DNA fragment (50 nM) and the TFO (at the indicated concentration) were incubated for 1 h at 30°C in a total volume of 10 μl of 50 mM Tris–HCl (pH 7.0), 120 mM KCl, 1 mM ATP, 10 mM $MgCl_2$, 0.5 mM DTT, 0.1 mM EDTA and 30 μg/ml of BSA in order to form the triplex or in the presence of the drug. Human topo IIα (0.7 U) was added to the triplex DNA and incubated for 20 min at 30°C. Following ethanol precipitation, samples were suspended in 6 μl of formamide, heated at 90°C for 3 min and chilled on ice for 4 min, they were then subjected to electrophoresis on a denaturing 8% polyacrylamide gel (19:1 acrylamide:bisacrylamide) containing 7.5 M urea in 1× TBE buffer (50 mM Tris-base, 55 mM boric acid, 1 mM EDTA) for 120 min at 65 W. To quantify the extent of cleavage, gels were scanned with a Typhoon 9410 (Amersham Biosciences). DNA cleavage was normalized to the total counts loaded in each reaction. Experiments were repeated between four and ten times.

Crosslinking assays

The 5′ end labeled 357 bp DNA fragment (50 nM) and the TFO (at the indicated concentration) were incubated for 1 h at 30°C in a total volume of 10 μl of 50 mM Tris–HCl (pH 7.0), 120 mM KCl, 1 mM ATP, 10 mM $MgCl_2$, 0.5 mM DTT, 0.1 mM EDTA and 30 μg/ml of BSA in order to form the triplex or in the presence of drug. Human topo IIα (0.7 U) was added to the DNA and incubated for 20 min at 30°C. All samples were irradiated at 365 nm for 30 min and reaction products were then treated in one of the three ways. (i) Direct analysis: samples were precipitated in ethanol. (ii) Piperidine cleavage reactions: piperidine (100 μl of a 1 M solution) was added to the reaction products and incubated at 90°C for 30 min. Piperidine was removed by lyophilization. (iii) DNase I footprinting: samples were digested with 1 μl of DNase I (final concentration 0.03 mg/ml, Sigma) diluted in 1 mM $MgCl_2$, 1 mM $MnCl_2$ and 20 mM NaCl (pH 7.3). The reaction was performed for 3 min at 20°C and was stopped by ethanol precipitation.

All samples subsequently were treated as in the topo II cleavage assay. DNA crosslinking was normalized to the total counts loaded in each reaction.

Competition experiments

The 5′ end 357 bp radiolabeled DNA fragment (50 nM) was incubated as above in the presence of the TFO (at the indicated concentration) in order to form the triplex or in the presence of the drug. Human topo IIα (0.7 U) was added to the samples and incubated at 30°C. After 5 min incubation, increasing concentrations (from 50 μM to 1 mM) of competitor (ICRF 193 or VP16) were added, and the incubation followed for other 15 min at 30°C. These samples, irradiated or not, were precipitated in ethanol and suspended in 6 μl of formamide. They were then subjected to electrophoresis on a denaturing 8% polyacrylamide gel (19:1 acrylamide:bisacrylamide) containing 7.5 M urea in 1× TBE buffer for 120 min at 65 W and analyzed as above. Experiments were repeated between four and ten times.

RESULTS

Experimental design

The target duplex contains a 20 bp oligopyrimidine•oligopurine sequence suitable for triplex formation (boldface in Figure 1). A 16mer triplex-forming ODN, 16TFO, containing 5-methyl-2′-deoxycytidine (M) and 5-propynyl-2′-deoxyuridine (P) was used in order to form a stable pyrimidine-motif triple helix at pH 7.0 (underlined sequence) (29–31). In order to verify the positioning of the drug by the triplex at different sites, the 16mer TFO was extended by 4 nt at its 3′ end to obtain 20TFO that forms a stable triple helix on the entire target sequence (in boldface). The drugs were attached either on the 5′ end or the 3′ end of the TFOs to explore also different sequence contexts.

The aim of the present study was to evaluate if triplex formation can be used to direct the action of topo II poisons and induce topo II-mediated DNA cleavage specifically at the triplex site. Therefore, the above TFOs were conjugated at their 3′ or 5′ end to four VP16 analogs (**1**, **2**, **3** and **4**), through a linker arm (Figure 1). Noteworthy, all analogs are derived from 4′-DMEP (4-β-demethylepipodophyllotoxin) by substitution of the C-4 position, and compounds **1**, **2** and **3** are very similar in structure. Compounds **1** and **3** are active topo II poisons that stabilize the topo II/DNA cleavage complexes and increase levels of DNA cleavage, while derivative **2** is inactive and was used as a control (22). Etoposide analogs were attached to TFOs via a primary amino group to the terminal phosphate of a hexaethylene glycol linker (L_{18}, $(OCH_2CH_2)_6PO_4^-$) at the end of the TFO, as described previously in (23). The carboxy derivative **4** was also shown to be a topo II poison and was linked to the TFO through a ethylene (L_3, $(OCH_2CH_2)PO_4^-$) or hexaethylene glycol (L_{18}) linker arm. Finally, two molecules of compound **4** were attached to the same terminal phosphate of the L_{18} linker arm, to the 3′ end of the TFOs (16TFO-L_{18}-$(4)_2$ and 20TFO-L_{18}-$(4)_2$), or to a trifunctional linker arm attached to the phosphate at the 3′ end of the 20TFO (20TFO-L_{12}-$(4)_2$). These latter constructs were designed to position two molecules of VP16 in the enzyme.

The chemical stability of all conjugates and their ability to form a triple-helical structure in the duplex target at pH 7.2 and 37°C was evaluated in a previous study (23).

A triple helix-mediated effect

In the first part of our study, the ability of the conjugates to induce topo II-mediated DNA cleavage was studied. Figure 2A shows the results obtained with analog **4** attached to the 16TFO through linker L_{18} either in 5′ (**4**-L_{18}-16TFO) or in 3′ (16TFO-L_{18}-**4**). As expected, **4** alone (lane 3) at 50 μM enhanced topo II-mediated DNA cleavage at several sites (e.g. e and h). The presence of a 16mer ODN at 1 μM, that differed in sequence from the 16TFO and was thus unable to bind to the target, did not modify the topo II cleavage profile (lane 4) or the one of **4** (lane 5). The triplex-specific 16TFO, once bound, mainly protected the triplex site from topo II-mediated DNA cleavage at sites c+d, for example, and enhanced cleavage at site b, at 11 bp from the 5′ triplex end, and slightly at site e, at 8 bp from the 3′ triplex end (lane 6). Furthermore, it did not inhibit the poisoning by **4** at the other sites (e and h, lane 7). When the 16TFO was attached at its 5′ end to the topo II poison, DNA cleavage was detected specifically at site a, situated 13 bp from the 5′ triplex end (lane 8). In contrast, cleavage at other sites were decreased (site e) or strongly decrease (sites c+d). Cleavage at site b, which was enhanced by triplex formation alone, was still observed. When compound **4** was attached to the 3′ end of the 16TFO, cleavage was observed primarily at site f, 14 bp from the 3′ triplex end, and weakly at site g, 18 bp from the 3′ end (lane 10). Sites c+d and e were strongly decreased, while site b, typical of the triplex structure was maintained. When the 16TFO-L_{18} and compound **4** were added unbound (lane 9), the sum of the cleavage profile of each partner was seen, similar to that obtained in the presence of L_{18}-16TFO and free **4** (lane 7).

These results suggest that the presence of the triple-helical structure influences the cleavage profile of topo II, probably by altering the local structure of DNA to which the enzyme is bound, as observed previously with TFO conjugates of amsacrine (20). Moreover, the TFO–DMEP conjugate is able to position the poison specifically at the end of the triplex and to stimulate sequence-specific topo II-mediated DNA cleavage. The 5′ conjugate directed topo II-mediated DNA cleavage specifically to the 5′ end of the triplex and, likewise, the 3′ conjugate to the 3′ end. When the sequence-specific DNA ligand was increased in length by 4 nt at its 3′ end (20mer 20TFO) and it was attached to **4** at its 3′ end through linker L_{18}, triplex-directed cleavage was observed mainly at site g, 14 bp from the 3′ triplex end (Figure 2B lane 7, and Supplementary Figure 1). As observed for the 16TFO, triplex formation protected the target site from topo II-mediated cleavage, and scission at sites c+d was abolished (compare lane 4 to lane 1, and Supplementary Figure 1). With this longer triplex, cleavage at site e was also strongly decreased even in the presence of unlinked **4** (lanes 5 and 6). Site b, characteristic of the triple-helical structure, is present on the 5′ side (lane 7). The addition of the free inhibitor changes the cleavage profile of the conjugate (lane 9) mainly by adding the cleavage sites of the free inhibitor, at the exclusion where the conjugate is bound as it is observed in the presence of the simple triplex, due to triplex protection from cleavage.

DNA cleavage also was observed on the opposite oligopurine-rich strand of the target duplex (Figure 2C), staggered by 4 bp, as expected for topo II-mediated DNA cleavage. The same cleavage profile was obtained.

The data are schematized in Figure 3A. Figure 3B summarizes the intensity of topo II-mediated DNA cleavage in the presence of the 20TFO-L_{18}-**4** conjugate. Supplementary Figure 1 shows two examples of denaturing gels that were used for quantitation. Data are normalized to the cleavage intensity induced by the free drug (at 1 μM) on a logarithmic scale at each cleavage site and on both strands of the duplex (in grey the oligopyrimidine strand, Y and in black the oligopurine strand, R). The conjugate (filled bars) is compared to the 20TFO-L_{18} alone (hatched bars). Clearly, cleavage is inhibited by the presence of the triple helix at sites c+d and e, while site g is strongly enhanced in the presence of the conjugate. The efficacy of cleavage is comparable on the two strands.

As was the case of the 16mer conjugate, enhanced cleavage was observed at site a when compound **4** was attached to the 5′ end of 20TFO (Figure 3A). This was expected because the two TFOs share the same 5′ end and differ only in length at the 3′ end.

All together, these data indicate that conjugation to a TFO directs the action of the topo II poison and induces site-specific topo II-mediated DNA cleavage.

Design of the conjugates

The choice of the linker arm between the poison and the TFO was directed by a molecular model obtained by docking the triple helix in the model of the interaction of topo II with DNA based on the crystal structure of yeast topo II and *Escherichia coli* gyrase (23). This study suggested that the hexaethylene glycol (L_{18}) was the best suited linker arm. As control a shorter tether was used, and compound **4** was attached to the 16TFO through an ethylene glycol (L_3), to obtain conjugate 16TFO-L_3-**4**. This conjugate was poorly active (data not shown). Thus, the hexaethylene glycol appears to be best suited to position the drug in its active site.

In order to validate the triplex-directed recruitment of topo II, three other derivatives of VP16 were examined (Figure 1): compounds **1** and **3**, which are active topo II poisons, and compound **2**, which is an inactive analog. These compounds were attached either to the 3′ or 5′ end of 16TFO; compound **1** also was attached to the 20mer TFO. The more efficient L_{18} was used as linker arm between the drug and the TFO. Interestingly, all compounds, **1**, **3** and **4**, shared the same cleavage sites, differing only in the intensity of cleavage (data not shown). The ratio of the cleavage intensity in the presence of the conjugate over the cleavage intensity of the poison alone is reported on a logarithmic scale as a function of the position on the target (Figure 3C). It appears that conjugation of the topo II poisons **4**, **1** and **3** to 16TFO and **4** and **1** to 20TFO directs topo II-mediated DNA cleavage specifically to the 5′ end of the TFO (site a), when attached at the 5′ end of the TFO, and to the 3′ end when attached to the 3′ end of the TFO (sites f and g, respectively). The inactive topo II poison **2**, which differs from compound **1** by the presence of a methyl group on the N-carbamate (Figure 1), remains poorly active when conjugated and displays a cleavage profile similar to that of the triplex helix alone. The cleavage efficacy

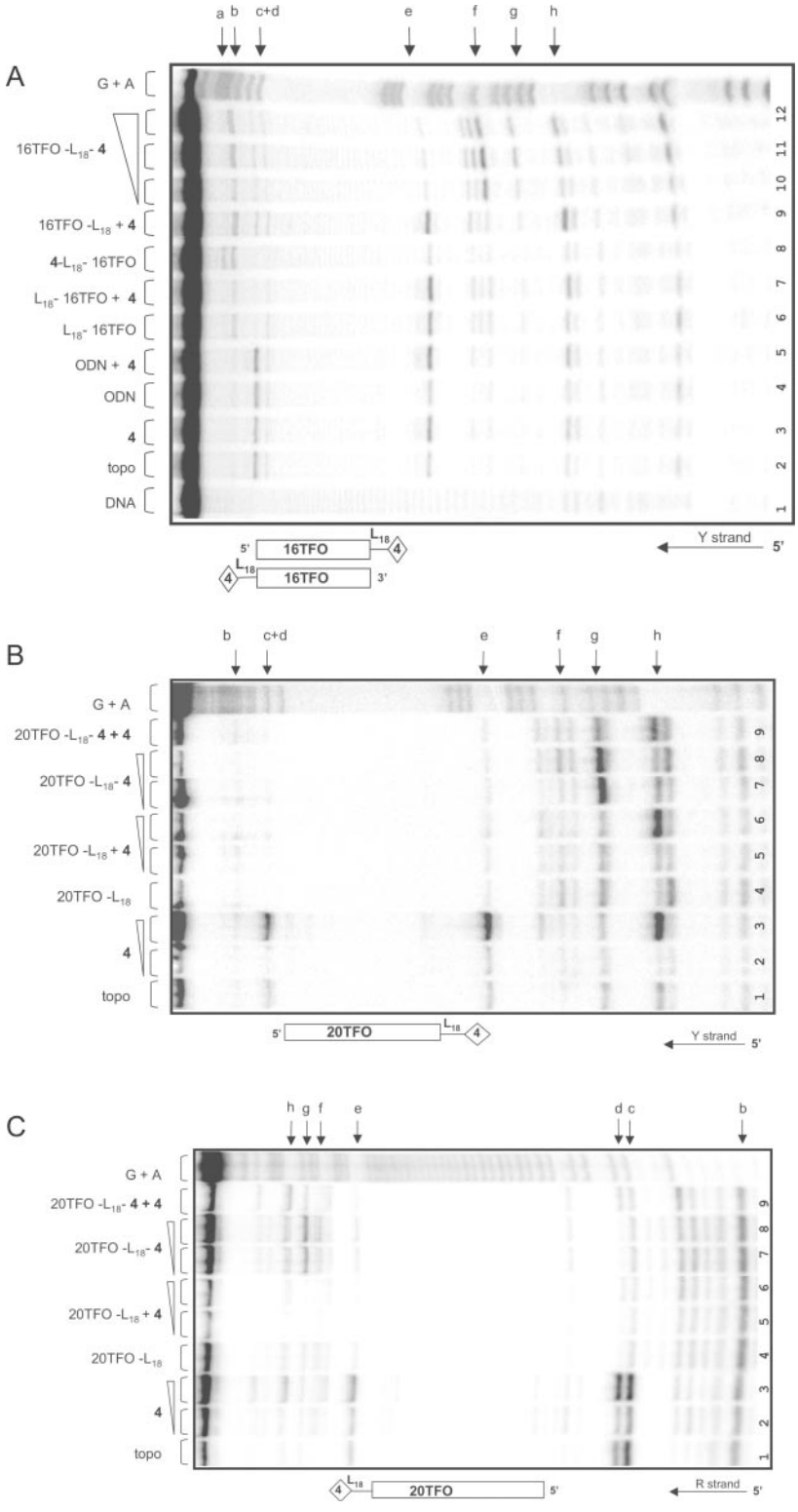

Figure 2. Sequence analysis of topo II-mediated cleavage products in the presence of the 16TFO-L_{18}-4, 4-L_{18}-16TFO and 20TFO-L_{18}-4 conjugates. This analysis was made on the 96 bp target duplex DNA (50 nM) that was 5′ end-radiolabeled on the oligopyrimidine-containing strand (**A** and **B**) or on the oligopurine-containing strand (**C**). Cleavage products were resolved on an 8% polyacrylamide gel containing 7 M urea. Adenine/guanine-specific Maxam–Gilbert chemical cleavage reactions were used as markers (lane G+A). The positions of the cleavage sites are indicated (sites a–h), together with the binding site of the TFO-conjugate. (A) Target duplex (lane 1) incubated with topo II (0.7 U) in the absence (lane 2) or presence of 50 μM 4 (lane 3), 1 μM ODN (lane 4), 1 μM ODN +50 μM 4 (lane 5), 1 μM L_{18}-16TFO (lane 6), 1 μM L_{18}-16TFO + 50 μM 4 (lane 7), 1 μM 4-L_{18}-16TFO (lane 8), 1 μM 16TFO-L_{18} + 50 μM 4 (lane 9), 0.5; 1 and 5 μM 16TFO-L_{18}-4 (lanes 10, 11 and 12). (B and C) Target duplex incubated with topo II (0.7 U) in the absence (lane 1) or in the presence of 1 μM (lane 2) or 50 μM 4 (lane 3), 1 μM 20TFO-L_{18} (lane 4), 1 μM 20TFO-L_{18} +1 μM 4 (lane 5), 1 μM 20TFO-L_{18} + 50 μM 4 (lane 6), 1 μM 20TFO-L_{18}-4 (lane 7), 5 μM 20TFO-L_{18}-4 (lane 8), 1 μM 20TFO-L_{18}-4 + 50 μM 4 (lane 9).

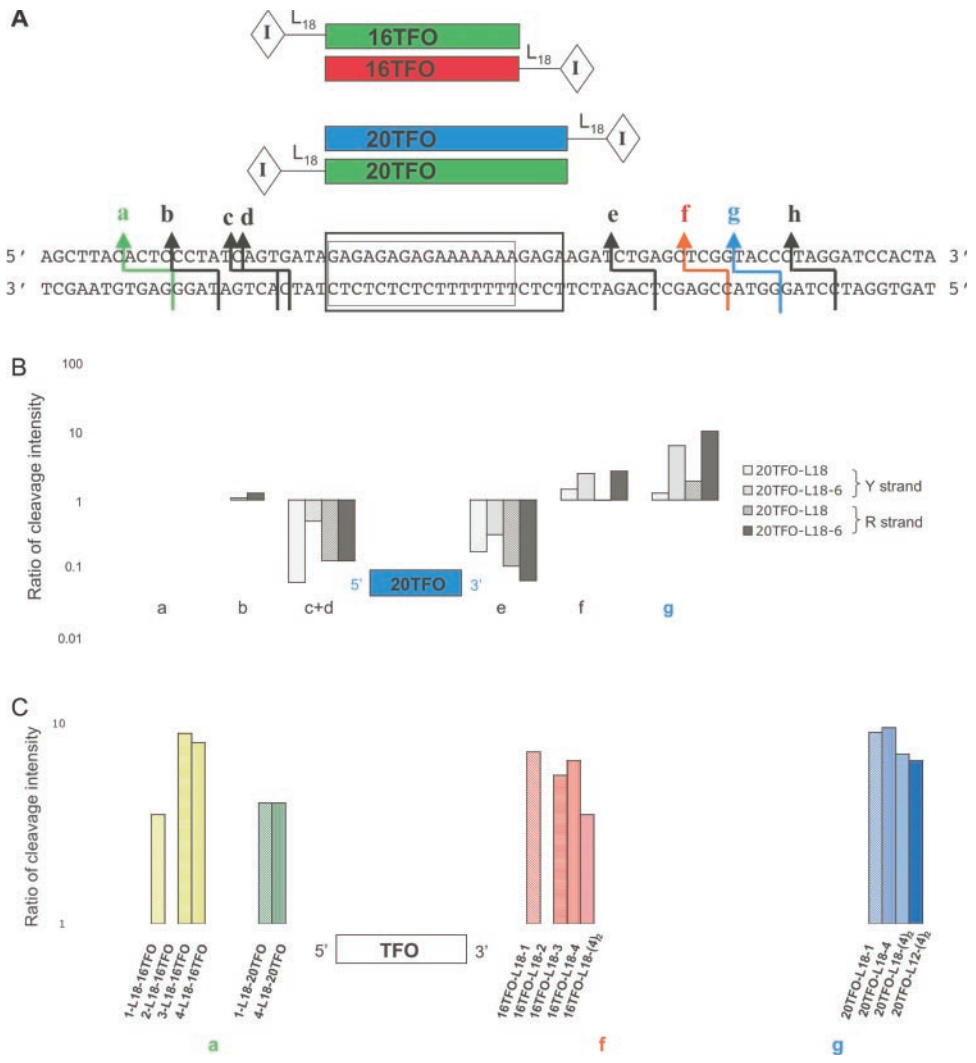

Figure 3. Quantification of topo II-mediated DNA cleavage in the presence of TFO–drug conjugates. The analysis was as in Figure 2 and the gels were quantified after normalization relative to total radioactivity loaded. (**A**) Scheme showing the enhanced cleavage site of each conjugate: the 5′ conjugates are depicted in green as the corresponding cleavage site a; the 3′ 16TFO conjugates are depicted in red as the corresponding cleavage site f; the 3′ 20TFO conjugates are depicted in blue as the corresponding cleavage site g. The other topo II-mediated DNA cleavage sites described in the text are also labeled with letters. (**B**) Quantification of the specific cleavage for 20TFO-L_{18}-**4** on both strands compared to free 20TFO-L_{18}. The cleavage intensity was normalized to the cleavage intensity of the free drug (at 1 μM) on a logarithmic scale at each cleavage site. The oligopyrimidine strand is in gray and the oligopurine strand is in black, the conjugate in filled bars and the 20TFO-L_{18} alone in hatched bars. (**C**) Specific cleavage intensities of the conjugates on the oligopyrimidine-containing strand of the duplex (Y). The 5′ 16TFO conjugates are depicted in light green (hatched bars **1**-L_{18}-16TFO, squares **2**-L_{18}-16TFO, horizontal bars **3**-L_s-16TFO, vertical bars **4**-L_{18}-16TFO), the 5′ 20TFO conjugates are depicted in dark green (hatched bars **1**-L_{18}-20TFO, vertical bars **4**-L_{18}-20TFO), the 3′ 16TFO conjugates are in red [hatched bars 16TFO-L_{18}-**1**, squares 16TFO-L_{18}-**2**, horizontal bars 16TFO-L_{18}-**3**, vertical bars 16TFO-L_{18}-**4**, crosses 16TFO-L_{18}-$(4)_2$] and the 3′ 20TFO ones are in blue [hatched bars 20TFO-L_{18}-**1**, vertical bars 20TFO-L_{18}-**4**, crosses 20TFO-L_{18}-$(4)_2$, dots 20TFO-L_{12}-$(4)_2$].

of the **1**, **3** and **4** conjugates is comparable at the 3′-end, but not at the 5′ end. Furthermore, at the 3′ end, the 20mer conjugates showed better cleavage efficacy compared to the 16mer conjugates.

The main triplex-induced cleavage site was unexpectedly situated 13–14 bp from the triplex end (site a, on the 5′ end, and site f, on the 3′ end for the 16TFO; Figure 3A). When the 16TFO was increased in length by 4 nt at its 3′ end to give the 20TFO, cleavage was induced by all 3′ 20mer conjugates 4 bp farther away, at site g. Because both TFOs share the same 5′ end, all 5′ conjugates stimulated cleavage at the same site a. In conclusion, whether the VP16 analogs were attached to the 3′ or the 5′ end of the TFO, the induced cleavage site was situated 13 or 14 bp from the end of the triplex and was observed on both strands of the duplex, with different intensities (Figure 3).

Another point to address is whether two poisons at the same TFO end induce a more efficient cleavage. Recently, it was demonstrated that the actions of VP16 at either of the two scissile bonds appear to be independent of one another, with each individual drug molecule stabilizing a strand-specific nick rather than a double-stranded DNA break (24). Thus, two drug molecules are necessary to observe cleavage on both strands. Double conjugates were synthesized (Figure 1) by covalent linkage of two molecules of **4** to the L_{18} linker at the 3′ end of both TFOs [16TFO-L_{18}-$(4)_2$ and 20TFO-L_{18}-$(4)_2$] or to two linkers at the 3′ end of the 20TFO [20TFO-L_{12}-$(4)_2$] (23). The three double conjugates induced

cleavage at the expected sites f and g, respectively, showing an efficiency slightly lower than the single conjugate (Figure 3C).

In brief, these results indicate that by conjugating a topo II poison to a TFO and binding of the conjugate to DNA, it is possible to position the drug at a specific and chosen site, and to stimulate topo II-mediated DNA cleavage at this site. However, the distance of the cleavage site from the triplex end, 13 and 14 bp, was unexpected. The longest linker used, hexaethylene glycol (L_{18}), is not long enough to position the drug at this distance. This raises the issue of where the conjugated topo II poison is actually positioned on the DNA.

Positioning of the TFO-poison conjugate in the ternary complex

Eukaryotic topo II is a homodimeric enzyme, that when bound to DNA covers ~25 bp symmetrically around the cleavage site (32–34). Furthermore, it is believed that drugs are positioned in the ternary complex at the topo II/DNA interface at the cleavage site (35). This has been demonstrated for mAMSA by the use of a photoactivable derivative that was crosslinked to DNA at the cleavage site in the presence of topo II (36). Clearly, the drug moiety of the TFO conjugates cannot realize this configuration.

To investigate the positioning of VP16 conjugate in relation to the scissile bonds, we modified compound **4** by reacting the 4′-OH group with an aromatic azido carboxylate. After deprotection of **5**, the resulting compound **6** was linked to the 3′ end of the TFOs through L_{18} (16TFO-L_{18}-**6** and 20TFO-L_{18}-**6**, Figure 4A). Compound **6** is still a topo II poison and shows the same cleavage pattern as the parent compound **4**, but has weaker activity (Figure 4B, lane 2). Because of the azido group, this conjugate is able to crosslink to DNA upon irradiation at 365 nm. By using the 20TFO-L_{18}-**6** and 16TFO-L_{18}-**6**

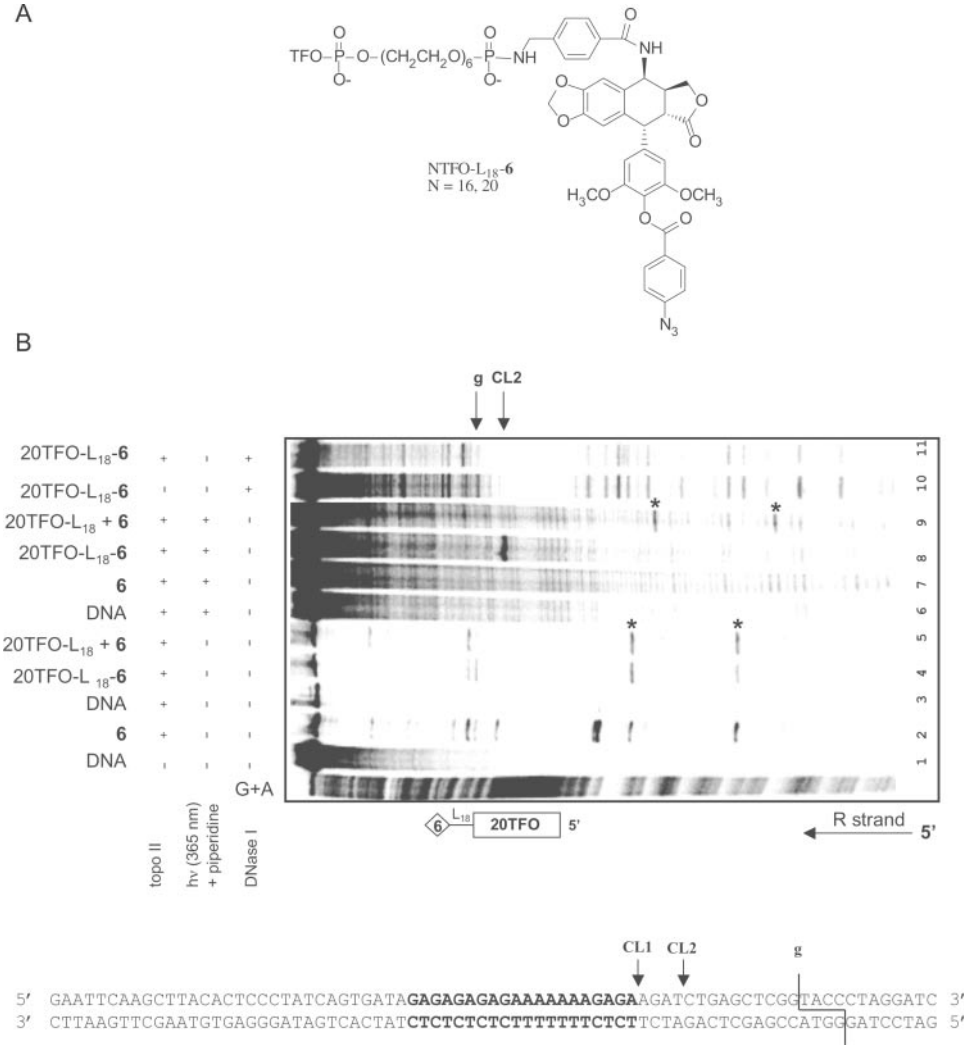

Figure 4. Crosslinking and DNase I footprinting experiments. (**A**) Chemical structure of conjugates bearing compound **6**. (**B**) Analysis of cleavage, crosslinking and DNase footprinting. The 357 bp target, 5′ radiolabeled on the oligopurine strand (lane 1) was incubated with topo II (lane 3) and in the presence of 50 μM **6** (lane 2), 1 μM 20TFO-L_{18}-**6** (lane 4) or 1 μM 20TFO-L_{18} + 50 μM **6** (lane 5), followed by UV radiation at 365 nm and piperidine treatement (lanes 6, 7, 8 and 9). Finally, DNase I was added after triplex formation with 1 μM of 20TFO-L_{18}-**6** (lane 10), followed by topo II addition (lane 11). Adenine/guanine-specific Maxam–Gilbert chemical cleavage reactions were used as markers (lane G+A). Positions of the cleavage site g and of the crosslinking site CL2 are indicated. Asterisks show the bands corresponding to cleavage or crosslinking of free compound **6** in the presence of the triplex. Arrows indicate the crosslinking positions of conjugates 16TFO-L_{18}-**6** (CL1) and 20TFO-L_{18}-**6** (CL2).

conjugates, we were able to determine the position of the drug on the DNA in the ternary complex. As depicted in Figure 4B, conjugate 20TFO-L_{18}-**6** induced topo II-mediated DNA cleavage at site g, as expected (lane 4). In contrast, the unbound 20TFO in the presence of an excess of **6** protected the triplex site from cleavage and did not modify the other cleavage sites (lane 5). Following irradiation and piperidine treatment, crosslinking was observed in the presence of the conjugate at site CL2, situated 4 bp from the triplex end (lane 8). This distance is in agreement with the length of the linker arm, 18 atoms. On average, 27% of the VP16 analog was crosslinked to the DNA. Crosslinking was only observed with the azido conjugates (Supplementary Figure 2). The presence of topo II was not necessary (Supplementary Figure 2, lanes 3 and 5), indicating that it is the triplex that positions the drug at this specific site, ready to trap the enzyme. In agreement, the cleavage activity of the enzyme was not necessary, as crosslinking also was observed in the presence of topo II Y805F (data not shown), mutated at the catalytic tyrosine necessary for the formation of the phosphotyrosyl bond involved in the DNA cleavage reaction. When compound **6** was conjugated to the 3′ end of 16TFO (16TFO-L_{18}-**6**), the crosslinking site again was observed at 4 bp from the triplex end (Supplementary Figure 2), site CL1 (Figure 4 lower).

To determine where the enzyme was situated on the DNA target in the presence of the conjugate, we compared DNase I footprinting experiments in the presence of the triplex formed by the conjugates in the absence and presence of topo II. Figure 4B shows an example of this analysis for conjugate 20TFO-L_{18}-**6**. Triplex formation protected the DNA from DNase cleavage at the triplex site (lane 10). In the presence of topo II, the footprint was extended on the 3′ side, to where the drug was positioned by the TFO (lane 11).

In summary, while the poison was located 4 bp from the triplex end, topo II-mediated DNA cleavage was induced 10 bp downstream from the site of drug crosslinking. In addition, topo II was symmetrically located around the cleavage site, as schematized in Figure 5A. Therefore, the positioning of the drug at the DNA/topo II interface at the catalytic site is excluded in this configuration.

DISCUSSION

Results of the present study demonstrate that topo II poisons can be directed to specific sequences by conjugating them to a TFO. In the case of VP16 analogs, DNA cleavage occurred in 14 bp from the end of the triplex site. Optimal cleavage was observed when the drug was conjugated with the hexaethylene glycol, L_{18}, linker arm and poisoning required an active drug analog.

These findings are similar to those reported for TFO-conjugated topo I poisons (18,37). However, topo I and II poisons differ from one another in two significant properties. First, while the conjugated VP16 analogs enhance topo II-mediated DNA scission when the drug is attached to either the 3′- or 5′-terminus of the TFO, conjugated camptothecin derivatives only increase topo I-mediated DNA scission when they are conjugated to the 3′-terminus of the TFO (38). Second, while the conjugated topo I poisons induce DNA cleavage in the vicinity of the drug, conjugated topo II poisons induce

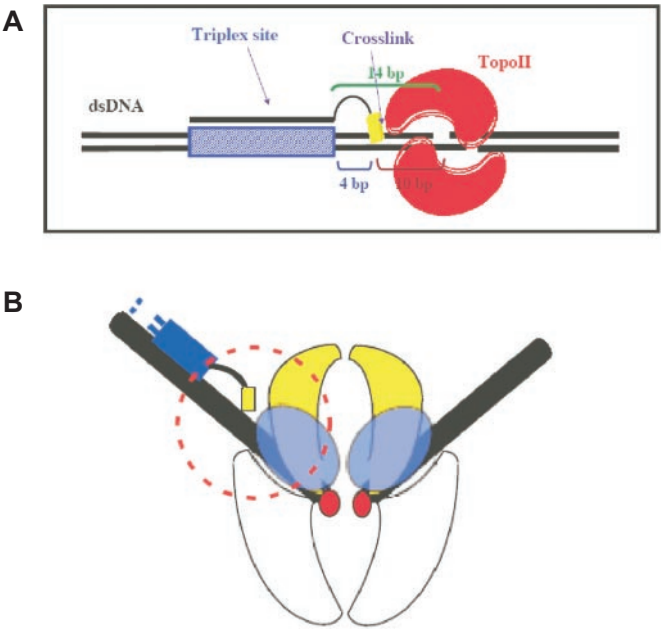

Figure 5. Model of interaction between TFO-conjugated topo II poisons and the enzyme. (**A**) Schematic positioning of the conjugated poison on the DNA duplex in the presence of topo II after the crosslinking and DNase I experiments. (**B**) Potential regions of contact between the conjugated poison and the enzyme are encircled in red. The various domains of the homodimer are schematically shown in red, white, light blue and yellow. The TFO is depicted in blue, the DNA duplex in black and the poison by a yellow rectangle.

cleavage more than one turn of the helix away from the triplex end. The length of the linker arm used to conjugate VP16 analogs to the TFO cannot position the drug at such a distance. In fact, by using an aromatic azido derivative, compound **6**, we showed that the drug moiety of the conjugate is located at 4 bp from the triplex end (summarized in Figure 5A).

Differences between the site of DNA cleavage and the location of the conjugated drug raise the question of where the poison interacts with the protein. Figure 5B depicts a model that schematically indicates the possible region of interaction of the drug with the protein. Since the poison in the conjugate is located too far away to interact directly at the catalytic site of topo II, we propose that it interacts in the B′A′ linker domain or at the edge of the A′ binding site, and thus acts by altering protein conformational changes associated with the topo II catalytic cycle. In agreement, several mutations in topo II that increase or decrease the sensitivity of the enzyme to anticancer drugs are positioned in the linker that joins the ATPase domain to module B′ and the B′A′ linker (39–43). Furthermore, our suggestion is in agreement with previous observations about several possible sites of interaction of VP16 on human topo IIα. According to previous reports (41,44), the drug has two binding sites in the protein: one in the catalytic site and one in the N-terminal, ATPase region of the enzyme.

Alternatively, it is possible that the ternary complex formed in the presence of the conjugates is very different from the one formed by the drug alone. Perturbations in the DNA induced by the triple-helical structure increased cleavage at specific site b (Figure 2). To this point, however, the conjugates induced cleavage at other specific sites (f, g and a). Additional

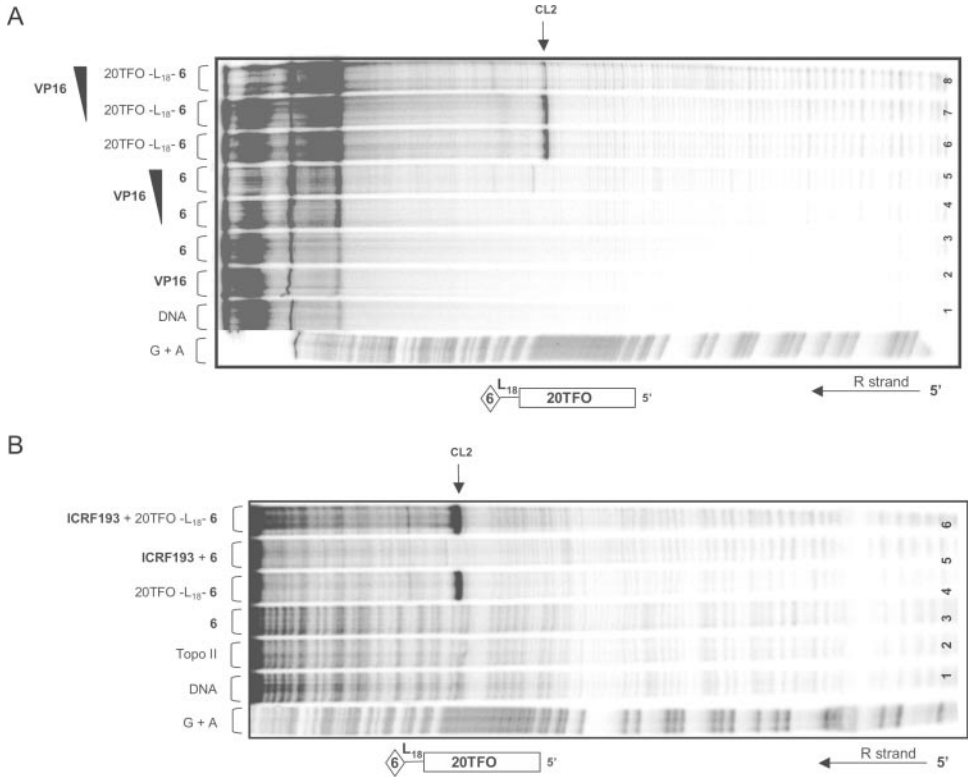

Figure 6. Crosslinking competition experiments. Experimental details as in Figure 4. Adenine/guanine-specific Maxam–Gilbert chemical cleavage reactions were used as markers (lane G+A). (**A**) Competition with VP16: 10 and 500 μM of VP16 were added to the 357 bp radiolabeled duplex target incubated with topo II in the presence of 50 μM **6** (lanes 4 and 5) or of 1 μM 20TFO-L_{18}-**6** (lanes 7 and 8), followed by UV radiation at 365 nm and piperidine treatement. As control, 500 μM **VP16** (lane 2), 50 μM **6** (lane 3) or 1 μM 20TFO-L_{18}-**6** (lane 6) was added alone in the presence of topo II. (**B**) Competition with ICRF193: 500 μM of ICRF193 was added to 50 μM **6** (lane 5) or 1 μM 20TFO-L_{18}-**6** (lane 6) after topo II addition, followed by UV radiation at 365 nm and piperidine treatement. As control DNA (lane 1) was incubated with topo II alone (lane 2) or in the presence of 50 μM **6** (lane 3) or 1 μM 20TFO-L_{18}-**6** (lane 4) prior to UV irradation.

sets of experiments suggest that the site of action of the conjugated poison is also a possible site of action the free poison on the enzyme. First, crosslinking experiments with free (i.e. non-conjugated) compound **6** were carried out. We observed that free compound **6** showed very weak crosslinking in the presence of topo II (Figure 4B, lane 7). In the presence of the enzyme and the triple helix, crosslinking is enhanced, and we observed that free compound **6** crosslinked to DNA 10 bp from the respective cleavage site, as in the case of TFO-conjugated compound **6**. This is shown in Figure 4B, lane 9: the crosslinking sites (asterisks) are shifted compared to the cleavage sites (lane 5, asterisks). These results suggest that even in the case of the non-conjugated drug **6** its cleavage site and its position on the DNA are 10 bp apart. Second, competition experiments between the drug–TFO conjugates and well-characterized topo II poisons (VP16) or catalytic inhibitors (ICRF193) were conducted (Figure 6). A 50-fold excess of VP16 (500 μM) strongly decreased the crosslinking efficiency of conjugated compound **6** (Figure 6A, lane 8), suggesting that the TFO-bound drug and VP16 compete for the same site. ICRF193 is a catalytic inhibitor that traps the enzyme in its stable clamp form around the DNA (45). This inhibitor did not compete with the crosslinking efficacy of conjugated compound **6** (Figure 6B, lane 6), suggesting that it does not share the same site of action (46).

Taken together, the above results suggest a large and/or flexible binding site for 4′-demethylepipodophyllotoxins on human topo IIα that may not be situated strictly in the catalytic site of the enzyme.

In conclusion, the use of triple helix-forming ODNs to target active topo II poisons, such as VP16, may be able to improve the efficacy of cancer chemotherapy by targeting topo II-induced cleavage to specific genes or genomic sequences. This approach has the potential to reduce the toxicity of VP16 and other topo II-active compounds and to overcome the undesired side effect these drugs, namely the induction of therapy-related leukaemia associated with chromosomal translocations involving *MLL* (12). Finally, TFO-conjugated topo II poisons represent a class of new tools that may help to unravel the mechanistic details of the complex process of topo II poisoning.

SUPPLEMENTARY DATA

Supplementary Data are available at NAR Online.

ACKNOWLEDGEMENTS

The authors thank Lionel Dubost and Dr Jean-Paul Brouard of the Mass Spectroscopy Service of the MNHN for the mass spectra analysis, and Prof. James M. Berger for helpful discussions. The authors are grateful to the referees for the helpful remarks. This work was supported by grants from Ligue

Nationale Contre le Cancer and ACI 'Molécules et Cibles thérapeutiques' du Ministère de la Recherche to P.B.A. and NIH grant GM33944 to N.O. D.G. was recipient of a fellowship from Fondation de France (Comité Leucémie), M.D. from ARC and K.O. from ARTP. Funding to pay the Open Access publication charges for this article was provided by INSERM.

Conflict of interest statement. None declared.

REFERENCES

1. Champoux,J.J. (2001) DNA topoisomerases: structure, function, and mechanism. *Annu. Rev. Biochem*, **70**, 369–413.
2. Wang,J.C. (2002) Cellular roles of DNA topoisomerases: a molecular perspective. *Nature Rev. Mol. Cell. Biol*, **3**, 430–440.
3. Wang,J.C. (1996) DNA topoisomerases. *Annu. Rev. Biochem*, **65**, 635–692.
4. Burden,D.A. and Osheroff,N. (1998) Mechanism of action of eukaryotic topoisomerase II and drugs targeted to the enzyme. *Biochim. Biophys. Acta*, **1400**, 139–154.
5. Capranico,G. and Binaschi,M. (1998) DNA sequence selectivity of topoisomerases and topoisomerase poisons. *Biochim. Biophys. Acta*, **1400**, 185–194.
6. Capranico,G., Zagotto,G. and Palumbo,M. (2004) Development of DNA topoisomerase-related therapeutics: a short perspective of new challenges. *Curr. Med. Chem. Anti-Canc. Agents*, **4**, 335–345.
7. Hande,K.R. (1998) Etoposide: four decades of development of a topoisomerase II inhibitor. *Eur. J. Cancer*, **34**, 1514–1521.
8. Hande,K.R. (2003) Topoisomerase II inhibitors. *Cancer Chemother. Biol. Response Modif*, **21**, 103–125.
9. Baldwin,E.L. and Osheroff,N. (2005) Etoposide, topoisomerase II and cancer. *Curr. Med. Chem. Anti-Canc. Agents*, **5**, 363–372.
10. Kaufmann,S.H. (1998) Cell death induced by topoisomerase-targeted drugs: more questions than answers. *Biochim. Biophys. Acta*, **1400**, 195–211.
11. Sordet,O., Khan,Q.A., Kohn,K.W. and Pommier,Y. (2003) Apoptosis induced by topoisomerase inhibitors. *Curr. Med. Chem. Anti-Canc. Agents*, **3**, 271–290.
12. Felix,C.A. (1998) Secondary leukemias induced by topoisomerase-targeted drugs. *Biochim. Biophys. Acta*, **1400**, 233–255.
13. Lovett,B.D., Lo Nigro,L., Rappaport,E.F., Blair,I.A., Osheroff,N., Zheng,N., Megonigal,M.D., Williams,W.R., Nowell,P.C. and Felix,C.A. (2001) Near-precise interchromosomal recombination and functional DNA topoisomerase II cleavage sites at MLL and AF-4 genomic breakpoints in treatment-related acute lymphoblastic leukemia with t(4;11) translocation. *Proc. Natl Acad. Sci. USA*, **98**, 9802–9807.
14. Lovett,B.D., Strumberg,D., Blair,I.A., Pang,S., Burden,D.A., Megonigal,M.D., Rappaport,E.F., Rebbeck,T.R., Osheroff,N., Pommier,Y.G. *et al.* (2001) Etoposide metabolites enhance DNA topoisomerase II cleavage near leukemia-associated MLL translocation breakpoints. *Biochemistry*, **40**, 1159–1170.
15. Whitmarsh,R.J., Saginario,C., Zhuo,Y., Hilgenfeld,E., Rappaport,E.F., Megonigal,M.D., Carroll,M., Liu,M., Osheroff,N., Cheung,N.K. *et al.* (2003) Reciprocal DNA topoisomerase II cleavage events at 5′-TATTA-3′ sequences in MLL and AF-9 create homologous single-stranded overhangs that anneal to form der(11) and der(9) genomic breakpoint junctions in treatment-related AML without further processing. *Oncogene*, **22**, 8448–8459.
16. Matteucci,M., Lin,K.-Y., Huang,T., Wagner,R., Sternbach,D.D., Mehrotra,M. and Besterman,J.M. (1997) Sequence-specific targeting of duplex DNA using a camptothecin-triple helix forming oligonucleotide conjugate and topoisomerase I. *J. Am. Chem. Soc*, **119**, 6939–6940.
17. Arimondo,P.B., Bailly,C., Boutorine,A., Sun,J.S., Garestier,T. and Hélène,C. (1999) Targeting topoisomerase I cleavage to specific sequences of DNA by triple helix-forming oligonucleotide conjugates. A comparison between a rebeccamycin derivative and camptothecin. *C R Acad. Sci. III*, **322**, 785–790.
18. Arimondo,P.B., Boutorine,A., Baldeyrou,B., Bailly,C., Kuwahara,M., Hecht,S.M., Sun,J.S., Garestier,T. and Hélène,C. (2002) Design and optimization of camptothecin conjugates of triple helix-forming oligonucleotides for sequence-specific DNA cleavage by topoisomerase I. *J. Biol. Chem*, **277**, 3132–3140.
19. Pommier,Y. (2004) Camptothecins and topoisomerase I: a foot in the door. Targeting the genome beyond topoisomerase I with camptothecins and novel anticancer drugs: importance of DNA replication, repair and cell cycle checkpoints. *Curr. Med. Chem. Anti-Canc. Agents*, **4**, 429–434.
20. Arimondo,P., Bailly,C., Boutorine,A., Asseline,U., Sun,J.S., Garestier,T. and Hélène,C. (2000) Linkage of a triple helix-forming oligonucleotide to amsacrine-4-carboxamide derivatives modulates the sequence-selectivity of topoisomerase II-mediated DNA cleavage. *Nucleosides Nucleotides Nucleic Acids*, **19**, 1205–1218.
21. Guianvarc'h,D., Duca,M., Boukarim,C., Kraus-Berthier,L., Leonce,S., Pierre,A., Pfeiffer,B., Renard,P., Arimondo,P.B., Monneret,C. *et al.* (2004) Synthesis and biological activity of sulfonamide derivatives of epipodophyllotoxin. *J. Med. Chem*, **47**, 2365–2374.
22. Duca,M., Guianvarc'h,D., Meresse,P., Bertounesque,E., Dauzonne,D., Kraus-Berthier,L., Thirot,S., Leonce,S., Pierre,A., Pfeiffer,B. *et al.* (2005) Synthesis and biological study of a new series of 4′-demethylepipodophyllotoxin derivatives. *J. Med. Chem*, **48**, 593–603.
23. Duca,M., Oussedik,K., Ceccaldi,A., Halby,L., Guianvarc'h,D., Dauzonne,D., Monneret,C., Sun,J.S. and Arimondo,P.B. (2005) Triple helix-forming oligonucleotides conjugated to new inhibitors of topoisomerase II: synthesis and binding properties. *Bioconjug Chem*, **16**, 873–884.
24. Bromberg,K.D., Burgin,A.B. and Osheroff,N. (2003) A two-drug model for etoposide action against human topoisomerase IIalpha. *J. Biol. Chem*, **278**, 7406–7412.
25. Pinney,K.G. and Katzenellenbogen,J.A. (1991) Synthesis of a tetrafluoro-substituted aryl azide and its protio analogue as photoaffinity labeling reagents for the estrogen receptor. *J. Org. Chem.*, **56**, 3125–3133.
26. Cantor,C.R., Warshaw,M.M. and Shapiro,H. (1970) Oligonucleotides interactions III. Circular dichroism studies of the conformation of deoxyoligonucleotides. *Biopolymers*, **9**, 1059–1077.
27. Grimm,G.N., Boutorine,A.S. and Hélène,C. (2000) Rapid routes of synthesis of oligonucleotide conjugates from non-protected oligonucleotides and ligands possessing different nucleophilic or electrophilic functional groups. *Nucleosides Nucleotides Nucleic Acids*, **19**, 1943–1965.
28. Arimondo,P., Boukarim,C., Bailly,C., Dauzonne,D. and Monneret,C. (2000) Design of two etoposide-amsacrine conjugates: topoisomerase II and tubuline polymerization inhibition and relation to cytotoxicity. *Anticancer Drug Des*, **15**, 413–421.
29. Froehler,B.C., Jones,R.J., Cao,X.D. and Terhorst,T.J. (1993) Oligonucleotides derived from 5-(1-propynyl)-2′-O- allyl-uridine and 5-(1-propynyl)-2'-O-allyl-cytidine: synthesis and RNA duplex formation. *Tetrahedron Lett.*, **34**, 1003–1006.
30. Lacroix,L., Lacoste,J., Reddoch,J.F., Mergny,J.L., Levy,D.D., Seidman,M.M., Matteucci,M.D. and Glazer,P.M. (1999) Triplex formation by oligonucleotides containing 5-(1-propynyl)-2′-deoxyuridine: decreased magnesium dependence and improved intracellular gene targeting. *Biochemistry*, **38**, 1893–1901.
31. Arimondo,P.B., Moreau,P., Boutorine,A., Bailly,C., Prudhomme,M., Sun,J.S., Garestier,T. and Hélène,C. (2000) Recognition and cleavage of DNA by rebeccamycin- or benzopyridoquinoxaline conjugated of triple helix-forming oligonucleotides. *Bioorg. Med. Chem*, **8**, 777–784.
32. Lee,M.P., Sander,M. and Hsieh,T. (1989) Nuclease protection by *Drosophila* DNA topoisomerase II. Enzyme/DNA contacts at the strong topoisomerase II cleavage sites. *J. Biol. Chem*, **264**, 21779–21787.
33. Spitzner,J.R., Chung,I.K. and Muller,M.T. (1990) Eukaryotic topoisomerase II preferentially cleaves alternating purine-pyrimidine repeats. *Nucleic Acids Res*, **18**, 1–11.
34. Thomsen,B., Bendixen,C., Lund,K., Andersen,A.H., Sorensen,B.S. and Westergaard,O. (1990) Characterization of the interaction between topoisomerase II and DNA by transcriptional footprinting. *J. Mol. Biol*, **215**, 237–244.
35. Capranico,G., Guano,F., Moro,S., Zagotto,G., Sissi,C., Gatto,B., Zunino,F., Menta,E. and Palumbo,M. (1998) Mapping drug interactions at the covalent topoisomerase II-DNA complex by bisantrene/amsacrine congeners. *J. Biol. Chem*, **273**, 12732–12739.
36. Freudenreich,C.H. and Kreuzer,K.N. (1994) Localization of an aminoacridine antitumor agent in a type II topoisomerase-DNA complex. *Proc. Natl Acad. Sci. USA*, **91**, 11007–11011.

37. Arimondo,P.B. and Hélène,C. (2001) Design of new anti-cancer agents based on topoisomerase poisons targeted to specific DNA sequences. *Curr. Med. Chem. Anti-Canc. Agents*, **1**, 219–235.
38. Arimondo,P.B., Angenault,S., Halby,L., Boutorine,A., Schmidt,F., Monneret,C., Garestier,T., Sun,J.S., Bailly,C. and Hélène,C. (2003) Spatial organization of topoisomerase I-mediated DNA cleavage induced by camptothecin-oligonucleotide conjugates. *Nucleic Acids Res*, **31**, 4031–4040.
39. Okada,Y., Ito,Y., Kikuchi,A., Nimura,Y., Yoshida,S. and Suzuki,M. (2000) Assignment of functional amino acids around the active site of human DNA topoisomerase IIalpha. *J. Biol. Chem*, **275**, 24630–24638.
40. Strumberg,D., Nitiss,J.L., Dong,J., Kohn,K.W. and Pommier,Y. (1999) Molecular analysis of yeast and human type II topoisomerases. Enzyme-DNA and drug interactions. *J. Biol. Chem*, **274**, 28246–28255.
41. Leroy,D., Kajava,A.V., Frei,C. and Gasser,S.M. (2001) Analysis of etoposide binding to subdomains of human DNA topoisomerase II alpha in the absence of DNA. *Biochemistry*, **40**, 1624–1634.
42. Gruger,T., Nitiss,J.L., Maxwell,A., Zechiedrich,E.L., Heisig,P., Seeber,S., Pommier,Y. and Strumberg,D. (2004) A mutation in *Escherichia coli* DNA gyrase conferring quinolone resistance results in sensitivity to drugs targeting eukaryotic topoisomerase II. *Antimicrob. Agents Chemother.*, **48**, 4495–4504.
43. Jiang,X. (2005) Random mutagenesis of the B′A′ core domain of yeast DNA topoisomerase II and large-scale screens of mutants resistant to the anticancer drug etoposide. *Biochem. Biophys. Res. Commun*, **327**, 597–603.
44. Vilain,N., Tsai-Pflugfelder,M., Benoit,A., Gasser,S.M. and Leroy,D. (2003) Modulation of drug sensitivity in yeast cells by the ATP-binding domain of human DNA topoisomerase IIalpha. *Nucleic Acids Res*, **31**, 5714–5722.
45. Classen,S., Olland,S. and Berger,J.M. (2003) Structure of the topoisomerase II ATPase region and its mechanism of inhibition by the chemotherapeutic agent ICRF-187. *Proc. Natl Acad. Sci. USA*, **100**, 10629–10634.
46. Ishida,R., Iwai,M., Hara,A. and Andoh,T. (1996) The combination of different types of antitumor topoisomerase II inhibitors, ICRF-193 and VP-16, has synergistic and antagonistic effects on cell survival, depending on treatment schedule. *Anticancer Res.*, **16**, 2735–2740.